

# Possible Parameters of Photon Colliders\*

Valery Telnov

Institute of Nuclear Physics, 630090, Novosibirsk, Russia

E-mail: telnov@inp.nsk.su or telnov@vxcern.cern.ch

## Abstract

Result of Monte Carlo simulation for photon colliders with "nominal" electron beam emittances (current designs) and for reduced horizontal emittances (by a factor 5) are presented. Two schemes are considered: with deflection of used beams after conversion by external magnetic field of 1 T and without deflection. It is shown that it is realistic to have  $\gamma\gamma$  luminosity at invariant masses  $W_{\gamma\gamma} / 2E_0 > 0.65$  about  $(3-5) \times 10^{33} \text{cm}^{-2}\text{s}^{-1}$  at  $2E_0 = 0.5$  TeV and up to  $10^{34}$  at  $2E_0 > 1$  TeV.

## 1 Introduction

General aspects of obtaining  $\gamma\gamma$ ,  $\gamma e$  colliding beams and their properties have been considered already in great details [1-6]. Last years there has been good progress in solid state and free-electron lasers and there are hopes that from this side there will be no serious limitations, therefore attainable luminosity of the photon colliders is limited only by coherent  $e^+e^-$  pair creation and, in principle, can be higher than that obtained with  $e^+e^-$  collisions. In order to obtain this high luminosity one needs  $e^-e^-$  beams (positrons are not necessary here) with high geometrical luminosity. The most valuable region for experiment is the high energy part of  $\gamma\gamma$  luminosity, where beside high energy there is high polarization and low background (for example  $\gamma\gamma \rightarrow$  Higgs signal does not disappear under  $\gamma\gamma \rightarrow b\bar{b}$  and  $\gamma g \rightarrow b\bar{b}$  backgrounds only with polarization and at the high energy end of the luminosity spectrum).

The  $\gamma\gamma$  luminosity in the region  $z = W_{\gamma\gamma} / 2E_0 > 0.65$  ( $W_{\gamma\gamma}$  is the invariant mass of two colliding photons) is equal approximately to 10% of geometrical  $e^-e^-$  luminosity (at conversion efficiency  $k \sim 0.65$ ). So, to obtain  $L_{\gamma\gamma} \sim L_{e^+e^-}$  one needs  $L_{ee}$  (geom.)  $\sim 10L_{e^+e^-}$ .

In  $e^+e^-$  collisions beams at interaction point (i.p.) should be flat in order to decrease beamstrahlung. For the present designs the aspect ratio  $\sigma_x/\sigma_y$  is about 20

\*The talk given at the International Workshop on Physics and Experimentation at Linear Colliders, Marioka-Appi, Japan, September 8, 1995

- 100. In photon colliders  $\sigma_x$  may be much smaller, but it is not easy to achieve. The minimum  $\sigma_x$  is determined by horizontal emittance of beam, which depends on the injector. Damping rings produce naturally flat beams with large ratio  $\epsilon_x/\epsilon_y$ . The first attempt to optimize final focusing systems for photon collisions has shown that maximum geometrical luminosity in this case is only about  $10^{34} \text{ cm}^{-2}\text{s}^{-1}$  for all projects, that means that  $L_{\gamma\gamma} (z > 0.65) \sim 10^{33} \text{ cm}^{-2}\text{s}^{-1}$ , That is by a factor 5 lower than  $e^+e^-$  luminosity [7],[6]. This is already satisfactory, keeping in mind that cross sections for charged pair production in  $\gamma\gamma$  collisions are by the same factor (5-10) larger than in  $e^+e^-$  collisions. Nevertheless the situation might be improved as is discussed below.

## 2 Beams emittances and sizes

In the present study I decided to consider again optimal focusing of beams for photon colliders including in the simulation code "Oide effect" (defocusing due to emission of synchrotron radiation photons in final lenses). Before this was taken in to account as gaussian addition, but in reality the number of emitted photons is small and their energy spectrum is very broad. Similar simulations were done also with horizontal emittance  $\epsilon_{nx}$  reduced by a factor 5. The hope that  $\epsilon_{nx}$  can be decreased by this factor is based on examination of limiting factors.

In damping rings  $\epsilon_{nx}$  is limited by 1) quantum fluctuations of synchrotron radiation and 2) intrabeam scattering. For the first effect, the equilibrium  $\epsilon_{nx}$  scales as  $E^3/N^3$ , where N is the number of bending magnets in the ring. Increasing the ring size by a factor 1.7 gives factor 5 improvement in  $\epsilon_{nx}$ . The damping time is determined by the strength of magnetic field and for large rings can be controlled by wigglers. The limit on emittance due to wigglers was found to be lower than our goal. The second effect, intrabeam scattering (IBS), beside many other parameters, depends on coupling between vertical and horizontal motion  $\zeta = \epsilon_{ny}/\epsilon_{nx}$  and equilibrium  $\epsilon_{nx} \text{ IBS} \propto 1/\sqrt{\zeta}$ . The vertical beam size in present designs is already very small and its further improvement for most of projects does not increase  $L_{\gamma\gamma}$ , therefore, for additional decreasing of  $\epsilon_{nx}$  one can also increase  $\zeta$  keeping  $\epsilon_{ny} = \text{const}$ . Estimations show that for this effect decrease of  $\epsilon_{nx}$  by a factor 5 is also possible.

In last years there is considerable progress in obtaining of low beam emittances with RF electron guns, which can be used as injector for photon colliders without damping rings. At the present the obtained emittance (product  $\epsilon_{nx} \epsilon_{ny}$ ) is by more than one order larger than necessary, but there are ideas how to improve it considerably.

## 3 Description of simulation conditions

The simulation code used in this study takes into account the following processes:

1. Multiple Compton scattering in the conversion region. In the present simulation "good" case of polarization ( $2P_e \lambda_e = -1$ ) [4,5] was taken and the thickness of the photon target was put equal to one conversion length. It was assumed (as first approximation) that polarization of the electrons does not change in Compton scattering.
2. Deflection by external magnetic field and synchrotron radiation in the region between conversion region and i.p..

For the case when there is no deflection the distance  $b$  between conversion region and i.p. was taken to be 0.3 cm. To reduce somewhat  $\gamma\gamma$  luminosity at low invariant masses due to beamstrahlung beams were separated vertically by  $0.25 \sigma_y$  (this help for beam repulsing).

For the case with deflection, the magnetic field  $B_e$  was assumed to be 10 kG and directed horizontally (used beams are deflected in vertical direction, where beam size is smaller). The distance between conversion region and i.p. was taken to be

$$b = \max(0.5 \text{ cm}, 1.5 \gamma \sigma_y, \sqrt{\frac{8 \sigma_y \gamma e}{r_e B_e}}, \sqrt{\frac{8 N \gamma^2 e r_e (1 - 0.5 k)}{\sqrt{2 \pi} \alpha B_e \sigma_z Y_b}})$$

Here the third term represents the deflection on the distance  $4 \sigma_y$ , the fourth term is connected with the coherent pair creation. The parameter  $Y_b \sim 1$  and was varied between 0.7-1.5 according to [5].

3. During beam collisions the electromagnetic forces, coherent pair creation and beamstrahlung were taken into account..

In the simulation the beams are described by about 1000 macroparticles strings of  $0.3 \sigma_x$  width and with the length of a slice  $0.04 \sigma_z$ . The code takes into account in a reasonable way also the Oide effect. It depends, of course, on details of focusing system, but not in a critical way. This was taken into account by assuming a somewhat higher effective magnetic field.

## 4 Results of simulation

Simulation was performed for nominal parameters of projects presented in Table 1 (except that both beams were electrons) and for horizontal emittances reduced by a factor 5. For each case the  $\beta$ -functions giving the maximum geometrical luminosity were used.

The results for the case without deflection are presented in table 2 and figs.1,3. The luminosity spectra (fig.1) are given both for "nominal" and reduced emittances for  $2E = 0.5, 1$  and  $2$  TeV while table 2 and fig.3 present only the results for nominal

emittances and the energy 0.5 and 1 TeV. The luminosity spectra are normalized on  $L = N^2 f / 4\pi\sigma_x\sigma_y$ , which is larger than real geometrical  $e^-e^-$  luminosity due to  $\beta$ -functions and Oide effect. Both "normalization" luminosity and real geometrical luminosities are given in tables.

The resulting total  $\gamma\gamma$  luminosity for the case without deflection is very large:  $2 \times 10^{34} - 10^{35} \text{ cm}^{-2}\text{s}^{-1}$ , but the region  $z > 0.65$  contributes only about 5%. It means that collisions at low invariant masses will produce large background due to many  $\gamma\gamma \rightarrow \text{hadr}$  events/per train collision (during resolution time of detectors). One can notice also that in fig.1 at  $2E = 2 \text{ TeV}$  the luminosity for VLEPP at high invariant masses is very low. This is due to the effect of coherent pair creation and can be fixed easily by increasing horizontal beam size (this is not done here, therefore the results for  $2E = 2 \text{ TeV}$  are show in table 2 and fig.3). Some decrease of  $\gamma\gamma$  luminosity at high energy is connected with normalization (due to Oide effect).

The results for the case with magnetic deflection of "used" beams are presented in tables 3,4 and figs.2,4. In this case the ratio  $L_{\gamma\gamma}(\text{total})/L_{\gamma\gamma}(z > 0.65) \sim 2.5-3$ , that is much better than without deflection, while values  $L_{\gamma\gamma}(z > 0.65)$  are almost equal in both cases.

As shown in fig.4 the reduction of horizontal emittance by a factor 5 increase  $L_{\gamma\gamma}(z > 0.65)$  by a factor of 2.2-2.5, somewhat better than the  $\sqrt{5}$  (if to assume  $\sigma_x \propto \sqrt{\epsilon_{nx}}$ ), due to reduction of Oide effect.

## 5 Conclusion

After reasonable decrease of horizontal emittance the luminosity of photon colliders will reach the level  $L_{\gamma\gamma}(z > 0.65) \sim (3-5) \times 10^{33} \text{ cm}^{-2}\text{s}^{-1}$  at  $2E = 500 \text{ GeV}$  and increase with the energy up to  $10^{34} \text{ cm}^{-2}\text{s}^{-1}$ .

As it was shown in [6] for low energy colliders ( $2E < 300-400 \text{ GeV}$  for NLC, JLC;  $< 750 \text{ GeV}$  for CLIC;  $< 900 \text{ GeV}$  for VLEPP and less than about 1 TeV for TESLA and SBLC) one can collide beams even with infinitely small transverse sizes. Due to repulsion beams are separated during the collision by rather large distance and coherent pair creation does not occur. In this energy region the  $L_{\gamma\gamma}(z > 0.65)$  above  $5 \times 10^{35} \text{ cm}^{-2}\text{s}^{-1}$  is possible for all projects. The two problems here still open are: how to obtain very small electron beam sizes and how to perform experimentation with about 100  $\gamma\gamma \rightarrow \text{hadr}$  events/collision.

In conclusion, the achieving  $L_{\gamma\gamma}(z > 0.65) \sim 5 \times 10^{33} - 10^{34}$  seems a reasonable and realistic goal for photon colliders.

## Acknowledgements

I would like to thank the LCWS95 organizing committee for the nice organiza-

tion of the workshop and the financial support. I am grateful to F.Richard (Orsay), J.-P. Delahaye and R.Corsini(CERN) for their hospitality during the preparation of this paper.

## References

- [1] I.Ginzburg, G.Kotkin, V.Serbo, V.Tel'nov, *Nucl.Instr. & Meth.* **205** (1983) 47.
- [2] I.Ginzburg, G.Kotkin, S.Panfil, V.Serbo, V.Tel'nov, *Nucl. Instr. & Meth.* **219** (1984)5.
- [3] V.Tel'nov, *Nucl.Instr.&Meth.A* **294** (1990)72.
- [4] D.Borden,D.Bauer,D.Caldwell, *SLAC-PUB-5715, UCSD-HEP-92-01.*
- [5] V.Tel'nov, *Proc.of Workshop on Gamma-Gamma Colliders*, Berkeley CA, USA, 1994, *Nucl.Instr.&Meth.A* **355**(1995)3.
- [6] V.Tel'nov, *Proc.of Workshop 'Photon 95'*, Sheffield, UK, April 1995,
- [7] K.-J.Kim, P.Pierini, A.Sesler, V.Tel'nov, *LC95*, KEK, Japan, March 1995.

Table 1: Some parameters of 0.5 TeV(c.m.)  $e^+e^-$  linear colliders

	TESLA	SBLC	JLC(X)	NLC	VLEPP	CLIC
$L, 10^{33} \text{cm}^{-2} \text{c}^{-1}$	6.	3.75	5.2	7.1	15.	7.
rep.rate,Hz	5	50	150	180	300	1800
# bunch/train	1130	125	85	90	1	10
part./bunch( $10^{10}$ )	3.6	2.9	0.63	0.65	20	0.8
$\sigma_x/\sigma_y(\text{nm})$	845/19	670/28	260/3	320/3.2	2000/4	247/7.4
$\sigma_z(\text{mm})$	0.5	0.5	0.09	0.1	0.75	0.2
$\Delta t$ bunch(ns)	708	16	1.4	1.4	-	0.66

Table 2:  $\gamma\gamma$  collisions at  $2E = 0.5$  and 1 TeV respectively without magnetic deflection. Number of particles in bunches, collision rate are as in Table 1. Beam emittances are "nominal" (as for  $e^+e^-$  collisions).

	TESLA	SBLC	JLC	NLC	VLEPP	CLIC
$\epsilon_{nx}/\epsilon_{ny}, \text{cm rad}$	14/0.25	10/0.5	3.3/0.048	5/0.05	20/0.075	3/0.15
$\beta_x/\beta_y, \text{mm}$	1/0.5	1/0.5	0.18/0.09	0.2/0.1	1.5/0.75	0.4/0.2
$\sigma_x/\sigma_y, \text{nm}$	170/16	140/23	35/3	45/3.2	250/11	50/7.8
conv.-IP dist.,cm	0.3	0.3	0.3	0.3	0.3	0.3
$L_g = N^2 f/4\pi\sigma_x\sigma_y, 10^{34}$	2.2	1.3	3.9	3.8	3.6	2.4
Lee ,(geom.)	1.7	1.05	1.9	1.95	2.9	1.8
(incl.eff.Oide and $\beta$ -func.)						
$L_{\gamma\gamma}, 10^{34}$	3.7	3.3	2.4	2.4	4.	2.8
$L_{\gamma\gamma} (z > 0.65)$	0.24	0.15	0.2	0.2	0.4	0.24
$L_{\gamma e}$ ,	1.2	1.8	1.6	1.7	0.67	1.6
$L_{\gamma e} (z > 0.6)$	0.23	0.28	0.35	0.4	0.14	0.38
$\vartheta_{x,max}/\vartheta_{y,max}, \text{mrad}$	7/8	7/7	7/7	7/8	14/15	5/7
$\beta_x/\beta_y, \text{mm}$	1/0.5	1/0.5	0.36/0.09	0.4/0.1	1.5/0.75	0.4/0.2
$\sigma_x/\sigma_y, \text{nm}$	120/11	100/16	35/2.1	45/2.3	180/7.6	35/5.5
conv.-IP dist.,cm	0.3	0.3	0.3	0.3	0.3	0.3
$L_g = N^2 f/4\pi\sigma_x\sigma_y, 10^{34}$	4.3	2.6	5.5	5.3	7.2	4.7
Lee ,(geom.)	3.1	1.8	2.7	2.6	5.1	2.7
(incl.eff.Oide and $\beta$ -func.)						
$L_{\gamma\gamma}, 10^{34}$	10.4	6.3	7.7	4.5	18	9.4
$L_{\gamma\gamma} (z > 0.65)$	0.5	0.3	0.45	0.3	0.65	0.4
$L_{\gamma e}$ ,	4.	2	4	2.8	2.2	5
$L_{\gamma e} (z > 0.6)$	4.9	3.5	0.58	0.57	0.15	0.66
$\vartheta_{x,max}/\vartheta_{y,max}, \text{mrad}$	6/6	5/6	6/6	4/5	15/18	5/5

Table 3:  $\gamma\gamma$  collisions at 2E = 0.5, 1 and 2 TeV respectively with vertical magnetic deflection (B = 1 T). Number of particles in bunches, collision rate are as in Table 1. Beam emittances are "nominal" (as for  $e^+e^-$  collisions).

	TESLA	SBLC	JLC	NLC	VLEPP	CLIC
$\epsilon_{nx}/\epsilon_{ny}$ , cm rad	14/0.25	10/0.5	3.3/0.048	5/0.05	20/0.075	3/0.15
$\beta_x/\beta_y$ , mm	1/0.5	1/0.5	0.18/0.09	0.2/0.1	1.5/0.75	0.4/0.2
$\sigma_x/\sigma_y$ , nm	170/16	140/23	35/3	45/3.2	250/11	50/7.8
conv.-IP dist., cm	1.17	1.66	0.7	0.68	1.87	0.72
$L_g = N^2 f/4\pi\sigma_x\sigma_y, 10^{34}$	2.2	1.3	3.9	3.8	3.6	2.4
$L_{ee}$ , (geom.)	1.7	1.05	1.9	1.95	2.9	1.8
(incl. eff. Oide and $\beta$ -func.)						
$L_{\gamma\gamma}, 10^{34}$	0.91	0.43	0.39	0.45	0.66	0.68
$L_{\gamma\gamma} (z > 0.65)$	0.2	0.12	0.13	0.14	0.19	0.18
$L_{\gamma e}$ ,	0.1	0.04	0.1	0.12	0.023	0.15
$L_{\gamma e} (z > 0.6)$	0.04	0.001	0.01	0.01	< 0.001	0.02
$\vartheta_{x,max}/\vartheta_{y,max}$ , mrad	2/5	1/3	1/3	1/3	2/9	1/3
$\beta_x/\beta_y$ , mm	1/0.5	1/0.5	0.36/0.09	0.4/0.1	1.5/0.75	0.4/0.2
$\sigma_x/\sigma_y$ , nm	120/11	100/16	35/2.1	45/2.3	180/7.6	35/5.5
conv.-IP dist., cm	1.71	2.35	1.34	1.29	3.5	1.06
$L_g = N^2 f/4\pi\sigma_x\sigma_y, 10^{34}$	4.3	2.6	5.5	5.3	7.2	4.7
$L_{ee}$ , (geom.)	3.1	1.8	2.7	2.6	5.1	2.7
(incl. eff. Oide and $\beta$ -func.)						
$L_{\gamma\gamma}, 10^{34}$	1.45	0.86	0.38	0.42	1.	1.15
$L_{\gamma\gamma} (z > 0.65)$	0.36	0.23	0.14	0.14	0.35	0.32
$L_{\gamma e}$ ,	0.12	0.05	0.04	0.06	0.01	0.2
$L_{\gamma e} (z > 0.6)$	0.002	< 0.001	0.001	< 0.001	< 0.001	0.02
$\vartheta_{x,max}/\vartheta_{y,max}$ , mrad	1/3	1/2	1/2	1/2	1/4	1/2
$\beta_x/\beta_y$ , mm	1/0.5	1/0.5	0.36/0.09	0.4/0.1	1.5/0.75	0.4/0.2
$\sigma_x/\sigma_y$ , nm	85/8	71/11	25/1.5	32/1.6	120/5.4	25/3.9
conv.-IP dist., cm	2.96	3.32	2.45	2.37	6.25	1.98
$L_g = N^2 f/4\pi\sigma_x\sigma_y, 10^{34}$	8.6	5.2	11	10.7	14.4	9.5
$L_{ee}$ , (geom.)	4.	2.8	3.3	2.8	8.3	4.
(incl. eff. Oide and $\beta$ -func.)						
$L_{\gamma\gamma}, 10^{34}$	1.9	1.15	0.35	0.36	1.2	1.1
$L_{\gamma\gamma} (z > 0.65)$	0.5	0.31	0.135	0.12	0.41	0.36
$L_{\gamma e}$ ,	0.09	0.04	0.03	0.02	0.015	0.12
$L_{\gamma e} (z > 0.6)$	< 0.001	< 0.001	0.001	< 0.001	< 0.001	0.002
$\vartheta_{x,max}/\vartheta_{y,max}$ , mrad	1/2	1/1	1/1	1/1	1/3	1/1

Table 4:  $\gamma\gamma$  collisions at  $2E = 0.5, 1$  and  $2$  TeV respectively with vertical magnetic deflection ( $B = 1$  T). Number of particles in bunches, collision rate are as in Table 1. Vertical beam emittance is "nominal" (as for  $e^+e^-$  collisions), but the horizontal one is reduced by factor 5.

	TESLA	SBLC	JLC	NLC	VLEPP	CLIC
$\epsilon_{nx}/\epsilon_{ny}, \text{cm rad}$	2.8/0.25	2/0.5	0.66/0.048	1/0.05	4/0.075	0.6/0.15
$\beta_x/\beta_y, \text{mm}$	1/0.5	1/0.5	0.18/0.09	0.2/0.1	1.5/0.75	0.4/0.2
$\sigma_x/\sigma_y, \text{nm}$	76/16	64/23	16/3	20/3.2	110/11	22/7.8
conv.-IP dist.,cm	1.17	1.66	0.7	0.68	1.87	0.72
$L_g = N^2 f/4\pi\sigma_x\sigma_y, 10^{34}$	4.8	2.9	8.7	8.4	8.05	5.3
$L_{ee}$ (geom.)	3.95	2.5	6.65	6.15	6.7	4.3
(incl.eff.Oide and $\beta$ -func.)						
$L_{\gamma\gamma}, 10^{34}$	1.8	0.75	0.77	0.94	1.19	1.2
$L_{\gamma\gamma} (z > 0.65)$	0.48	0.28	0.35	0.34	0.42	0.43
$L_{\gamma e}$	0.19	0.045	0.16	0.19	0.27	0.26
$L_{\gamma e} (z > 0.6)$	0.01	0.001	0.025	0.02	< 0.001	0.05
$\vartheta_{x,max}/\vartheta_{y,max}, \text{mrad}$	1/5	1/3	1/3	1/3	2/9	1/3
$\beta_x/\beta_y, \text{mm}$	1/0.5	1/0.5	0.18/0.09	0.2/0.1	1.5/0.75	0.4/0.2
$\sigma_x/\sigma_y, \text{nm}$	53/11	45/16	11/2.1	14/2.3	78/7.6	16/5.5
conv.-IP dist.,cm	1.71	2.35	1.34	1.29	3.5	1.06
$L_g = N^2 f/4\pi\sigma_x\sigma_y, 10^{34}$	9.6	5.8	17	17	16.1	10.6
$L_{ee}$ (geom.)	7.8	4.7	9.7	9.6	13	7.9
(incl.eff.Oide and $\beta$ -func.)						
$L_{\gamma\gamma}, 10^{34}$	3.1	1.5	0.75	0.86	1.73	2.3
$L_{\gamma\gamma} (z > 0.65)$	0.93	0.56	0.36	0.37	0.75	0.82
$L_{\gamma e}$	0.18	0.05	0.1	0.1	0.02	0.37
$L_{\gamma e} (z > 0.6)$	0.005	<0.001	0.001	<0.001	< 0.001	0.04
$\vartheta_{x,max}/\vartheta_{y,max}, \text{mrad}$	1/3	1/2	2/4	~1/2	1/5	2/2
$\beta_x/\beta_y, \text{mm}$	1/0.5	1/0.5	0.18/0.09	0.2/0.1	1.5/0.75	0.4/0.2
$\sigma_x/\sigma_y, \text{nm}$	38/8	32/11	7.8/1.5	10/1.6	55/5.4	11/3.9
conv.-IP dist.,cm	2.96	3.32	2.45	2.37	6.25	1.98
$L_g = N^2 f/4\pi\sigma_x\sigma_y, 10^{34}$	19.	12	35	33.7	32	21
$L_{ee}$ (geom.)	13	8.45	12.5	11.5	25	13
(incl.eff.Oide and $\beta$ -func.)						
$L_{\gamma\gamma}, 10^{34}$	4	2.6	0.76	0.96	2.4	2.5
$L_{\gamma\gamma} (z > 0.65)$	1.4	0.95	0.4	0.5	1.	1.1
$L_{\gamma e}$	0.12	0.05	0.03	0.04	0.03	0.19
$L_{\gamma e} (z > 0.6)$	< 0.001	0.001	0.001	0.004	0.001	0.003
$\vartheta_{x,max}/\vartheta_{y,max}, \text{mrad}$	1/2	1/1	1/2	1/1	2/5	1/2



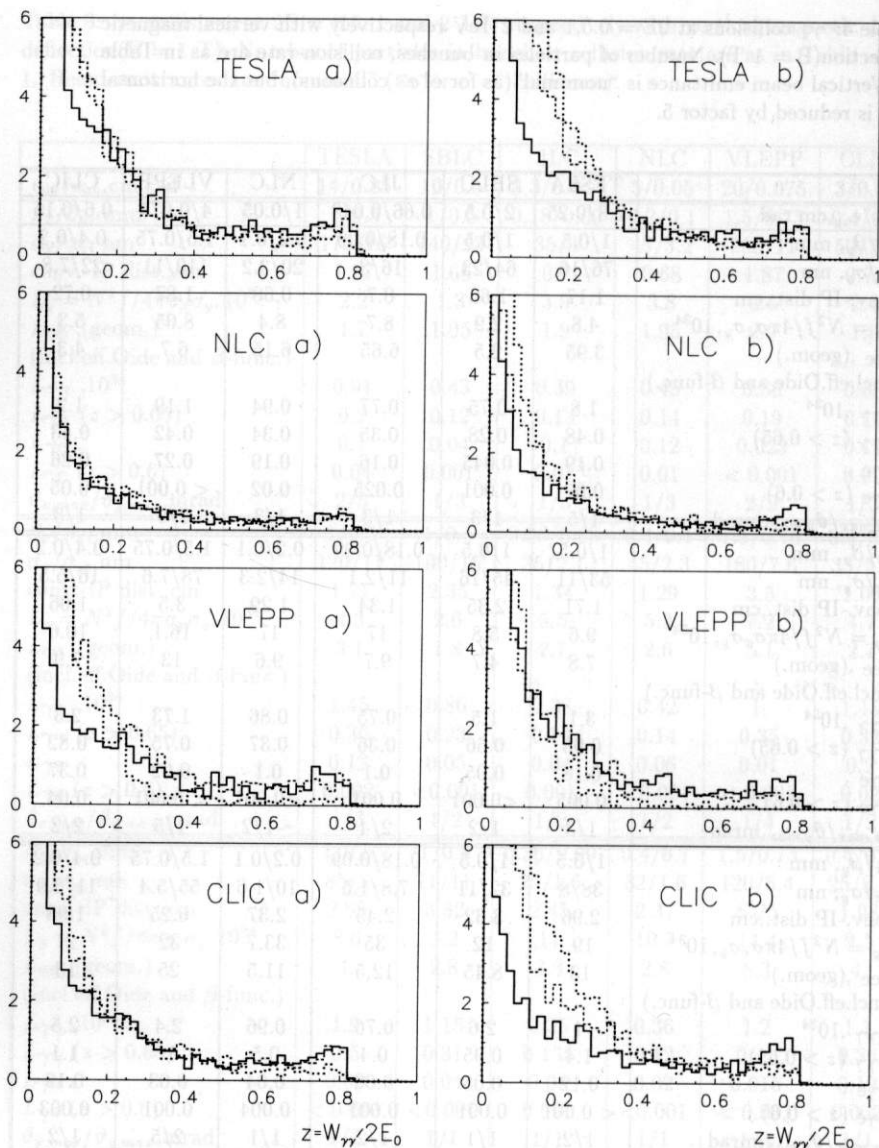


Fig. 1  $L_{\gamma\gamma}$  distributions for the scheme without magnetic deflection. Solid lines— $2E = 500$  GeV, dashed — 1000 GeV, dotted — 2000 GeV; figs. a) for “nominal” emittances, b) — for horizontal emittance reduced by a factor 5. The luminosities are normalized on  $L = N^2 f / 4\pi\sigma_x\sigma_y$ . The histograms for JLC and SBLC are not shown. They are close to NLC and TESLA respectively (results for all projects are presented in tables).

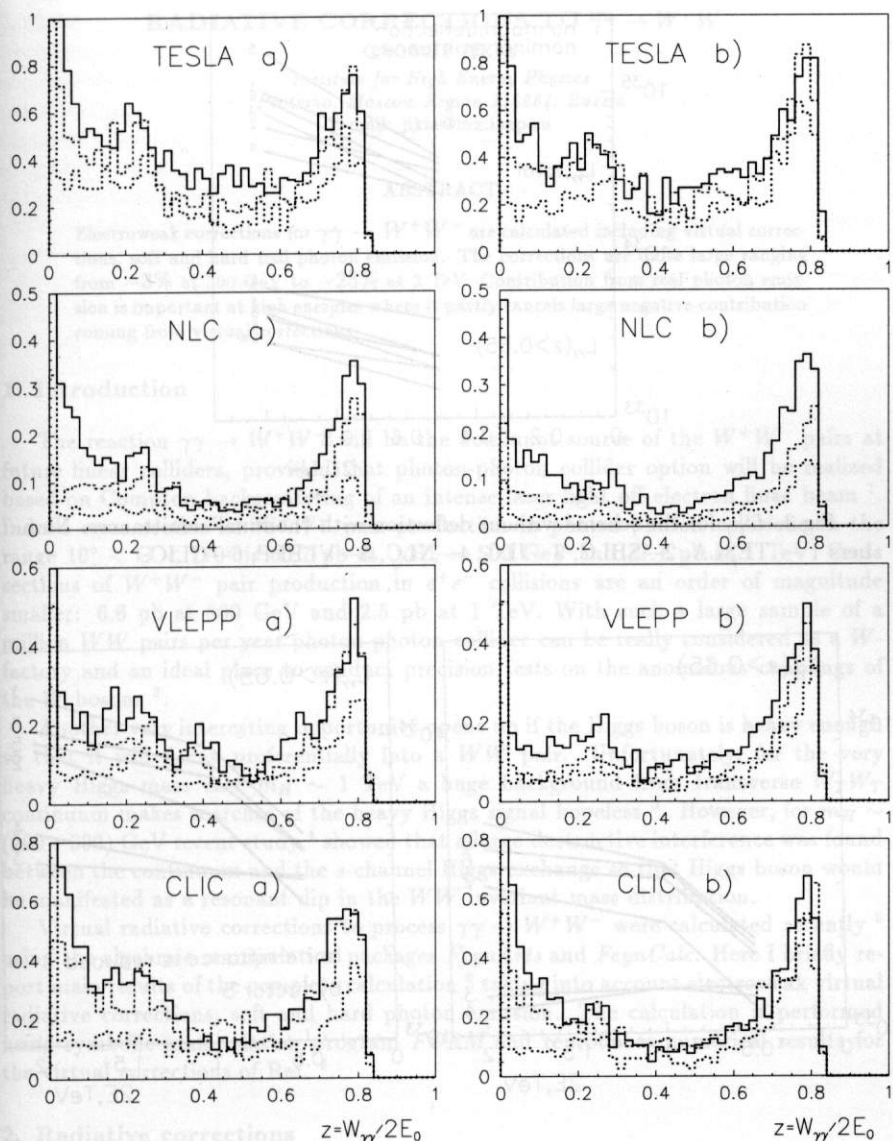


Fig. 2  $L_{\gamma\gamma}$  distributions for the scheme with magnetic deflection. Solid lines— $2E = 500$  GeV, dashed — 1000 GeV, dotted — 2000 GeV. figs.a) for “nominal” emittances, b) - for horizontal emittance reduced by a factor 5. The luminosities are normalized on  $L = N^2 f / 4\pi\sigma_x\sigma_y$ . The histograms for JLC and SBLC are not shown. They are close to NLC and TESLA respectively (results for all projects are presented in tables).

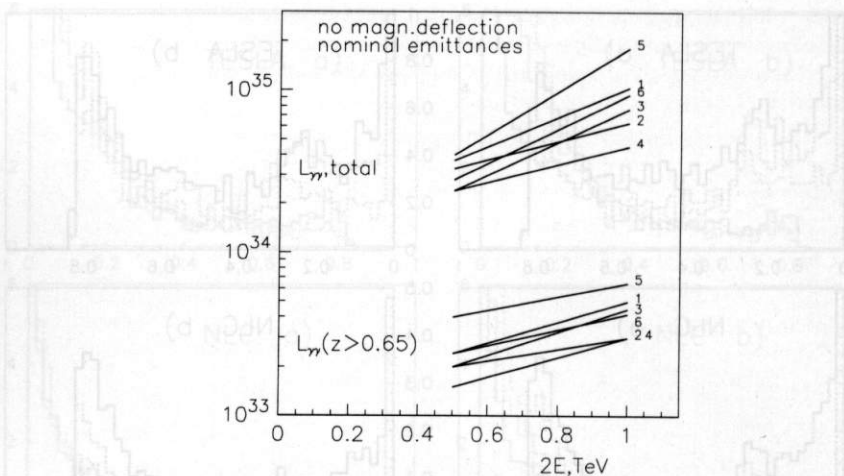


Fig.3.  $L_{\gamma\gamma}$  for the scheme without deflection with "nominal" emittances. Numbers 1 — TESLA, 2—SBLC, 3—JLC, 4—NLC, 5—VLEPP, 6—CLIC.

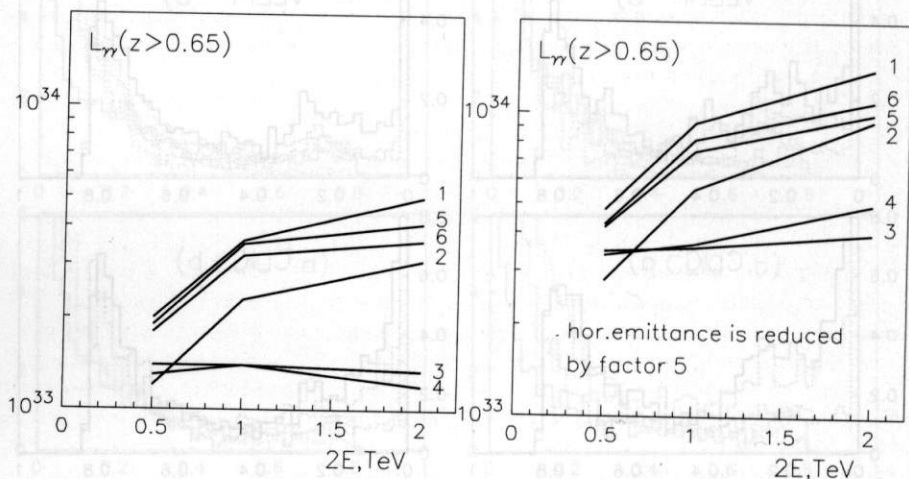


Fig.4.  $L_{\gamma\gamma}$  for the scheme with magnetic deflection with "nominal" emittances (left figs.) and reduced by a factor 5 horizontal emittances (right). Numbers 1 — TESLA, 2—SBLC, 3—JLC, 4—NLC, 5—VLEPP, 6—CLIC.